A comparative study of numerical schemes for the Baer-Nunziato model

Sophie Dallet[†⋆]

[†] *EDF R&D, MFEE, 6 quai Watier - 78400 CHATOU - FRANCE*

[⋆] *Institut de Mathématiques de Marseille, UMR CNRS 7373, 39 rue Joliot Curie - 13453 MARSEILLE - FRANCE*

sophie.dallet@edf.fr

Abstract

The present paper is devoted to a comparison of numerical methods for the convective part of a two-phase flow model. Four explicit schemes are tested using Riemann problems or smooth solutions. The main criteria for comparing the methods are: the accuracy for a fixed size of mesh, the convergence, the robustness and the CPU time cost necessary to reach a fixed error. The conclusions of this study are the following. The classical Rusanov scheme is not competitive, as expected. The relaxation scheme seems to be more efficient than the VFROE-ncv method, especially regarding robustness. The staggered scheme, recently investigated for this model, is sometimes less accurate for a fixed size of mesh than the VFROE-ncv and relaxation schemes but is the most acurate for a fixed run time.

Key words : Baer-Nunziato model, benchmark study, explicit schemes.

1 Introduction

Within the context of water-steam flows simulation for civil nuclear applications, the simulation of a two-fluid model introduced by Baer and Nunziato [3] is considered. There is no general agreement about the modeling of such flows, and from a general point of view about two phase flows modeling. Since the compressibility of fluids is still considered, the fluid may be described using several kinds of model: the homogeneous one - which uses the same velocity and pressure for both phases - or the two-fluid one. The homogeneous models are Euler-type models with specific closure laws. Two-fluid models are composed of two systems of PDEs - one for each phase - coupled through non-conservative interfacial terms and relaxation source

terms. Since the pressures are chosen equal in the whole space-time domain in the two-fluid model, the eigenvalues of the Jacobian matrix are not always real and thus the Cauchy problem is not uniquely solvable.

We consider thus a two-fluid model - the Baer-Nunziato model - where pressures are not assumed equal. There are several versions of this one, in particular with different choices of interfacial velocity and pressure ([23], [10], [12]). Extensions to a porous medium [11] and to multi-phase flows with three or more phases ([15], [14],[20]) have been made. In this paper we will only consider the initial model: the interfacial velocity is the velocity of one of the phases while the interfacial pressure is the pressure of the other phase.

The set of equations of the model is composed of a convective part and source terms: relaxation terms and external forces. The relaxation source terms may be very stiff, and from a numerical point of view they can be handled in different ways:

- A first way to deal with stiff source terms is to use asymptotic-preserving (AP) schemes: such schemes must be built in an ingenious way in order to ensure consistency with the asymptotic model when relaxation time scales - included in relaxation terms - vanish. This kind of scheme ensures an accurate approximation if source terms are stiff, but depends on modelling choices. This is still an open problem for the whole Baer-Nunziato model, while a first AP scheme has been developped for the barotropic version of this model [1].

- A more common way of proceeding is to use a splitting method for the source terms (see [17] for the model considered and [18] for the general framework): for each time iteration, convection and source terms are resolved successively. It is thus necessary that the Cauchy problem for the convective part has a solution. This is ensured by the fact that the convective part is strictly hyperbolic, except when resonance occurs, which is a specific case that cannot happen in our applications. This kind of method is very convenient: it only requires a solver for the convective part, for which there are a lot of schemes ([22], [10], [7], [17] which will be tested in this paper, but also [9], [24], [2], [25] this list is not exhaustive), and source terms solvers. This modular method is very useful from an industrial point of view. Naturally it is expected that the convective solvers be accurate and robust.

  In this study the stability, the accuracy and the CPU times - which is important from an industrial point of view - of several numerical schemes for the convective part of the Baer-Nunziato model are thus compared and their convergence is checked.

The outline of the paper is as follows. First the governing equations and the properties of the model are mentioned. Then some elements to build exact solutions - a smooth solution and Riemann problems - are given. Next, comparative tests are done, with ideal gas (IG) equation of state (EOS) for the two phases in the first

instance and then with stiffened gas (SG) equation of state for one phase and IG EOS for the other one. Finally we will conclude on the results.

2 The Baer-Nunziato model

Assuming one-dimensional flow, the equations of the convective part of the Baer-Nunziato (BN) model [3] are as follows:

$$\frac{\partial \alpha_2}{\partial t} + V_I \frac{\partial \alpha_2}{\partial x} = 0 \tag{1}$$

$$\frac{\partial}{\partial t}(\alpha_k \rho_k) + \frac{\partial}{\partial x}(\alpha_k \rho_k u_k) = 0 \tag{2.k}$$

$$\frac{\partial}{\partial t}(\alpha_k \rho_k u_k) + \frac{\partial}{\partial x}(\alpha_k \rho_k u_k^2) + \frac{\partial}{\partial x}(\alpha_k P_k) - P_I \frac{\partial \alpha_k}{\partial x} = 0 \tag{3.k}$$

$$\frac{\partial}{\partial t}(\alpha_k \rho_k E_k) + \frac{\partial}{\partial x}(\alpha_k \rho_k E_k u_k + \alpha_k P_k u_k) + P_I \frac{\partial \alpha_k}{\partial t} = 0 \tag{4.k}$$

Statistical fractions α_k are such that $0 < \alpha_k < 1$ and $\alpha_1 + \alpha_2 = 1$.

ρ_k, u_k, P_k and E_k ($k = 1$ or 2) denote the density, the velocity, the pressure and the total energy of the kth phase. The last one is defined by:

$E_k = e_k + \frac{1}{2}u_k^2$ where e_k denotes internal energy of the kth phase.

The pressure of each phase is given by different equations of states: $P_k = \mathcal{P}_k(\rho_k, e_k)$. In this article we assume ideal or stiffened gases EOS for each phase:

$P_k = (\gamma_k - 1)\rho_k e_k$ with $\gamma_k > 1$ (IG)
$P_k = (\gamma_k - 1)\rho_k e_k - \gamma_k P_{k,0}$, with $P_{k,0}$ a given positive constant and $\gamma_k > 1$ (SG).

The interfacial velocity and pressure are chosen as follows:
$(V_I, P_I) = (u_1, P_2)$ or $(V_I, P_I) = (u_2, P_1)$

The sound velocities c_k are defined by $c_k^2 = \frac{1}{\partial_{P_k}(e_k)}\big(\frac{P_k}{\rho_k^2} - \partial_{\rho_k}(e_k)\big)$

In particular, for IG or SG EOS the sound velocity can be written:

$$c_k = \sqrt{\frac{\gamma_k P_k}{\rho_k}} \quad \text{(IG)} \qquad\qquad c_k = \sqrt{\frac{\gamma_k (P_k + P_{k,0})}{\rho_k}} \quad \text{(SG)}$$

Some well-known properties of this model are reminded:

Property 1 *The system (1-4) is weakly hyperbolic. The seven real eigenvalues are:*

$\lambda_1 = V_I \quad \lambda_2 = u_1 + c_1 \quad \lambda_3 = u_1 - c_1 \quad \lambda_4 = u_2 + c_2 \quad \lambda_5 = u_2 - c_2 \quad \lambda_6 = u_1 \quad \lambda_7 = u_2$

The associated eigenvectors span the whole space $\mathbb{R}^7$ *unless* $|u_2 - u_1| = c_l$*, where* l *is the phase such that* $P_I := P_l$*.*

The characteristic fields associated with eigenvalues $\lambda_{1,6,7}$ *are linearly degenerate while the fields associated with eingenvalues* $\lambda_{2,3,4,5}$ *are genuinely nonlinear.*

The phasic entropies $s_k(P_k, \rho_k)$ are defined by $c_k^2 \partial_{P_k}(s_k) + \partial_{\rho_k}(s_k) = 0$

The choice of (V_I, P_I) is important to define jump conditions across the wave associated with λ_1 [10].

PROPERTY 2 *The following entropy equality holds for smooth solutions:*

$$\partial_t\Big(\sum_{k=1,2}(m_k s_k)\Big) + \partial_x\Big(\sum_{k=1,2}(m_k u_k s_k)\Big) = 0$$

where $m_k = \alpha_k \rho_k$*. The introduction of viscous contributions [13] and source terms [19] enables to derive an entropy inequality that reads:*

$$\partial_t\Big(\sum_{k=1,2}(m_k s_k)\Big) + \partial_x\Big(\sum_{k=1,2}(m_k u_k s_k)\Big) \geq 0$$

The source terms correspond to pressure, velocity, temperature, Gibbs potential relaxation effects. Recall that temperature and velocity relaxation are associated with heat exchange between phases and drag effects respectively. Gibbs potential unbalance is responsible of mass transfer.

3 Exact solutions

In this section some elements are given to build a smooth solution when both EOS are ideal gases, then a reminder concerning the method of construction of solutions to Riemann problems is given.

3.1 Smooth solution manufacturing

We have been interested in testing the schemes using a smooth solution. The following proposition is dedicated to the building of some smooth solutions. The meaning of the proposition is the following: for some specific given properties of the solution, what are the initial conditions that allow these expected properties?

The main idea is to find a basic solution with constant (in time and in space) material velocities. Short enough times are considered so that perturbations stay away from boundaries.

PROPOSITION 3.1

Let $\overline{T} > 0$, $x_0 < x_1$ given real numbers.

Let $W : (x,t) \mapsto W(x,t) = [w_i(x,t)]_{i\in[\![1;7]\!]} \in \mathcal{C}^1([x_0,x_1]\times[0;\overline{T}[,]0;1[\times(\mathbb{R}_*^+)^4\times\mathbb{R}^2)$ such that:

- $\forall t \in [0;\overline{T}[\ \ \forall i \in [\![1;5]\!] \quad x \longmapsto \partial_x(w_i(x,t)) \in \mathcal{C}_c^0(]x_0,x_1[)$
- $w_6(x,t) = \overline{w_6} \in \mathbb{R}\ \ \forall (x,t) \in [x_0,x_1]\times[0;\overline{T}[$
- $w_7(x,t) = \overline{w_7} \in \mathbb{R}\ \ \forall (x,t) \in [x_0,x_1]\times[0;\overline{T}[$

Let (BN_IG) the system (1-4) - which unknown is $\mathcal{W} = [\alpha_2,\rho_1,\rho_2,P_1,P_2,u_1,u_2]$ - closed with $V_I = u_1$, $P_I = P_2$, Dirichlet boundary conditions and ideal gas equations of states for both phases: $P_k = (\gamma_k - 1)\rho_k e_k$.

If there exists $T \in [0;\overline{T}[$ such that $W_{|_{[x_0,x_1]\times[0,T]}}$ be a solution of (BN_IG) then initial conditions are given by:

$$\begin{array}{l} \alpha_2(x,0) = \overline{\alpha_0} \\ m_k(x,0) = \overline{m_k}(x) \text{ for } k = 1,2 \\ P_k(x,0) = \overline{P_k} \text{ for } k = 1,2 \\ u_k(x,0) = \overline{u_k} \text{ for } k = 1,2 \end{array} \qquad \textit{(Type 1)}$$

or, if $\overline{w_6} = \overline{w_7}$:

$$\begin{array}{l} \alpha_2(x,0) = \overline{\alpha}(x) \\ m_k(x,0) = \overline{m_k}(x) \text{ for } k = 1,2 \\ P_2(x,0) = \overline{P_2} \\ P_1(x,0) = \dfrac{p_0}{1-\overline{\alpha}(x)} + \overline{P_2} \\ u_1(x,0) = u_2(x,0) = \overline{u_1} \end{array} \qquad \textit{(Type 2)}$$

where $\overline{\alpha_0} \in]0,1[$, $\overline{u_1} = \overline{w_6}$, $\overline{u_2} = \overline{w_7}$, $\overline{P_1} > 0$ $\overline{P_2} > 0$ and $p_0 > -\overline{P_2}\big(1-\max\limits_x(\overline{\alpha}(x))\big)$ are real constants. $\overline{\alpha}$ (resp $\overline{m_k}$, for $k = 1,2$) is a smooth function of one real variable defined on $\mathbb{R}$ to $]0;1[$ (resp $\mathbb{R}_*^+$) whose derivative is a function with compact support on $]x_0;x_1[$.

Moreover, the solutions for $(x,t) \in [x_0,x_1]\times[0;T]$ are thus:

$$\begin{array}{l} \alpha_2(x,t) = \overline{\alpha_0} \\ m_k(x,t) = \overline{m_k}(x - \overline{u_k}t) \text{ for } k = 1,2 \\ P_k(x,t) = \overline{P_k} \text{ for } k = 1,2 \\ u_k(x,t) = \overline{u_k} \text{ for } k = 1,2 \end{array} \qquad \textit{(Type 1)}$$

or:

$$
\begin{aligned}
&\alpha_2(x,t) = \overline{\alpha}(x - \overline{u_1}t) \\
&m_k(x,t) = \overline{m_k}(x - \overline{u_1}t) \text{ for } k = 1,2 \\
&P_2(x,t) = \overline{P_2} \\
&P_1(x,t) = \frac{p_0}{1 - \overline{\alpha}(x - \overline{u_1}t)} + \overline{P_2} \\
&u_1(x,t) = u_2(x,t) = \overline{u_1}
\end{aligned}
\qquad \textit{(Type 2)}
$$

It is easy to check that these functions are solutions of the system. The proof of the proposition is not more difficult and is left to the reader.

We are not interested in type 1 solutions because the fraction is constant. We will consider type 2 solutions (see test 5.1.1). Notice that compatibility conditions are needed: equality of velocities and also an equation between P_1, P_2 and α_k.

Remark 1 It is possible to generalize type 2 solutions with discontinuous $\overline{\alpha}(x)$ or $\overline{m_1}(x)$ if ρ_2 is continuous. Indeed, the assumptions $u_1(x,t) = u_2(x,t) = \overline{u_1} \in \mathbb{R}$, $P_2(x,t) = \overline{P_2} \in \mathbb{R}$ and the continuity of ρ_2 ensure jump conditions at a contact discontinuity compatible with $P_1(x,t) = \dfrac{p_0}{1 - \overline{\alpha}(x - \overline{u_1}t)} + \overline{P_2}$.

3.2 Solutions of Riemann problems

Some elements to build solutions of Riemann problem are given in this section. The solution of a Riemann problem is composed of constant states separated by shock waves, rarefaction waves or contact discontinuities. We set $V_I = u_1$ and $P_I = P_2$. Eingenvalues are thus:

$$\lambda_{1,6} = u_1 \text{ (double)} \quad \lambda_2 = u_1 + c_1 \quad \lambda_3 = u_1 - c_1 \quad \lambda_4 = u_2 + c_2 \quad \lambda_5 = u_2 - c_2 \quad \lambda_7 = u_2$$

Unlike the Euler equations, waves are not naturally ordered, we just know a priori that $\lambda_3 < \lambda_{1,6} < \lambda_2$ and $\lambda_5 < \lambda_7 < \lambda_4$. Consequently to build a Riemann problem and its solution, it is easier to start from a left state and to cross each wave successively to obtain intermediate states and right state than to start from left and right states and resolve the Riemann problem.

Notice that except for the wave associated with $\lambda_{1,6}$ the two phases evolve independently: the solution for each phase is locally that of the Euler equations. The wave's parametrisation is the same as the single-phase case:

- As the fields associated with $\lambda_{2,3,4,5}$ are genuinely nonlinear, each wave can be a shock wave or a rarefaction wave. The shock waves are thus built using Ranking-Hugoniot jump relations and complying with Lax entropy criterion, while the rarefaction waves are parametrized by the Riemann invariants.

- The field associated with λ_7 is linearly degenerate. The discontinuity is parametrized using the same Riemann invariants as the Euler equations: u_2 and P_2.

The field associated with $\lambda_{1,6}$ is linearly degenerate. It is typical of this model and permits the coupling between the two phases. The discontinuity associated is parametrized by the following Riemann invariants:

$$I^1_{1,6} = u_1 \qquad I^2_{1,6} = m_2(u_1 - u_2) \qquad I^3_{1,6} = m_2 u_2(u_2 - u_1) + \alpha_1 P_1 + \alpha_2 P_2$$

$$I^4_{1,6} = m_2(u_1 - u_2)\Big(e_2 + \frac{P_2}{\rho_2} + \frac{1}{2}(u_1 - u_2)^2\Big) \qquad I^5_{1,6} = s_2$$

Notice that the previous smooth solution preserves these invariants.

4 Numerical schemes

Four numerical schemes have been tested on several benchmark tests. The first one is the classical Rusanov scheme (see [21] for the historical approach, then [17] for the adaptation to the BN model). The second one is a VFROE-ncv scheme (see [4] for the general approach and [10] for the BN case with the same set of non-conservative variables). The third one is a relaxation approximation (see [6] for the barotropic case and [5] for the model with energy equations). The last scheme [7], called BN_SSIEE and described in appendix A, uses discretisations of the internal energy equations instead of the total energy ones and a staggered mesh for the velocities. This scheme is adapted from a scheme previously developed for the Euler equations [16].

Some properties of these schemes are reminded:

4.1 Rusanov scheme

The main idea of the Rusanov (or local Lax-Friedrichs) finite volume scheme is to use a centred flux to which enough dissipation is added to ensure the stability. The viscosity coefficient included in the numerical fluxes is chosen as the maximum absolute value of the local wave speeds, that makes the scheme very diffusive. The fluxes are then easily evaluated, and the CPU time is low since the maximum absolute values of the local wave speeds are memorized when the time step is evaluated. The positivity of the void fraction and the partial masses is ensured by CFL-like conditions.

4.2 VFROE-ncv scheme

The VFROE-ncv scheme is an approximate Godunov scheme. The main idea of this scheme is to solve exactly an approximate linear system to evaluate the fluxes of a finite volume scheme.

First, an admissible change of variables is adopted: $Q = [\alpha_2, u_1, u_2, P_1, P_2, s_1, s_2]$. The model is then written using this new set of variables:

$$\partial_t(Q) + B(Q)\partial_x(Q) = 0$$

At the n^{th} time iteration and at the interface $i+\frac{1}{2}$, $B(Q)$ is approximated by $B(Q)^n_{i+\frac{1}{2}}$ using Q^n_i and Q^n_{i+1}. The following system is then resolved exactly:

$$\partial_t(Q) + B(Q)^n_{i+\frac{1}{2}}\partial_x(Q) = 0$$

As all fields are linearly degenerate, this system is easy to solve, but the considerable number of computed approximate wave speeds makes this scheme more costly (in CPU time) than the Rusanov scheme.

At last, interfacial approximations Q^* are used to compute the fluxes of a finite volume scheme (in conservative variables).

4.3 Relaxation scheme

The relaxation scheme is a finite volume scheme based on the Suliciu approach. This scheme [5] has been extended from the barotropic version [6] of the relaxation scheme using Entropy-Energy duality. A larger system in which the pressures have been linearized is firstly introduced. This relaxation system, which depends on a relaxation parameter, tends to the convective part of the BN model when this parameter tends to 0. The first step of the algorithm is to solve the Riemann problem of the homogeneous relaxation system; that requires a fixed-point resolution. The second step consists in an instantaneous relaxation sending instantaneously this parameter to 0. The relaxation scheme is an entropy-satisfying scheme which preserves the positivity of the statistical fractions, the densities and the pressures (for ideal gas EOS) under a CFL-like condition. Moreover it has been recently proved that the specific enthalpies remain positive for stiffened gas EOS.

4.4 BN_SSIEE scheme

The BN_SSIEE scheme (see appendix A) is an extension to the Baer-Nunziato model of a scheme proposed in [16] for the Euler equations. A staggered mesh is used to define the velocities. The internal energy equations are discretized instead of the total energy equations. A corrective term is then "added" in the discretizations of the internal energy equations to offset a residual term that appears in the discrete kinetic energy balances in order to converge to the expected solution. The fluxes are easily (and low costly in CPU time) computed since they are approximated by the upwinding technique (with respect to the material velocity and not with respect to the wave velocities) or by the centered technique. The statistical fractions remain between 0 and 1, the densities, the specific enthalpies (at least for ideal or stiffened gas EOS) remain positive under CFL-like conditions.

4.5 General comments

Regular meshes are used for all the tests (for colocated schemes and the staggered scheme, for which the center of dual cells is located at the border of primal ones'). The time step is computed for all schemes using:

$$\Delta t^n = \frac{CFL}{\max_{i,k} \left(|u_k| + c_k\right)_i^n} \times h \tag{2}$$

It is convenient to mention for the following simulations that a parameter concerning the accuracy of a fixed-point resolution (a dichotomy) has to be fixed for the relaxation scheme unlike the other schemes. The choice of this parameter affects the results (accuracy, CPU time). We have chosen to fix this parameter - named ϵ - constant for each test, independently of the mesh size. ϵ is chosen small enough so that the error related to the fixed point resolution would be small with respect to the concistency error on the finest meshes. CPU times obtained on coarse meshes should thus be shorter if ϵ is bigger, but it doesn't seem to be really sensitive in actual pratice.

Notice that the results are obtained using unidimentional codes. The VFROE-ncv, Rusanov and BN_SSIEE schemes have been programed using FORTRAN 95 unlike the relaxation scheme has been programed using C. CPU times obtained may be thus affected.

5 Test cases and numerical results

In this section, several test cases are considered. First, ideal gas laws are considered for the two phases. The first test case is the simulation of a smooth solution. The following ones are Riemann problems. The second test is a λ_1-isolated contact wave. The solution of the third test case contains two shock waves and a λ_1-contact discontinuity.
Then a stiffened gas law is considered for one of the phases and an ideal gas law is considered for the other one. Two test cases have been carried out: a stationary contact discontinuity and another Riemann problem which includes all the waves.

The notation X_{disc} refers to the initial position of the discontinuity of the Riemann problem.

Whenever possible and useful the study of the schemes' convergence with respect to mesh refinement has been performed. The convergence curves are plotted using the logarithm to base 10 and L^1 discrete errors have been normalized. These curves show:

$Log_{10}\Big(\frac{||s_a - s_e||_{L^1}}{||s_e||_{L^1}}\Big)$ as a function of $Log_{10}(h)$

with s_a the approximate solution obtained with a space step h and s_e the exact solution.

The CPU time T_{CPU} between the beginning and the end of time iterations of each simulation has been measured. Each simulation has used an unique processor (the same for every computations). It is important to notice that measured CPU times are meaningless if considered alone, because depending on the processor used: it is the ratio between CPU times obtained for the different schemes which is significant. Numerical results show:

$Log_{10}(T_{CPU})$ as a function of $Log_{10}\Big(\frac{||s_a - s_e||_{L^1}}{||s_e||_{L^1}}\Big)$

We must remark that some CPU times obtained for Rusanov and BN_SSIEE schemes with the coarsest meshes are not very significant due to the shortness of these times and the lack of accuracy of very short CPU times measurements. We must also note that the ratio between CPU times obtained for Rusanov and those obtained for VFROE-ncv may differ significantly according to the test: most of the CPU time of VFROE-ncv is used for the computation of interfacial states, and the cost of those ones depends on the pattern of the waves of the linearized problem (simple upwinding or many root computations).

The parameter ϵ of the relaxation scheme has been set to 10^{-9} for the tests 1, 2, 3 and to 10^{-6} for the tests 4 and 5.

5.1 Ideal gas - Ideal gas

In this part, the equations of state are the following:

$$P_k = (\gamma_k - 1)\rho_k e_k \text{ with } \gamma_k > 1$$

5.1.1 Test 1: A smooth solution

A type-2 solution (see section 3.1) is considered. The following property concerning approximate solutions obtained with Rusanov and BN_SSIEE schemes holds:

Let M^n be a connected set of cells of the (primal) mesh, not necessarily regular, such that for each mesh of this set the approximation of the variables at the n^{th} iteration is independent of boundary conditions (ie those cells are far enough from the boundary). Let M_D^n be the largest set of dual cells such that the volume covered by those cells is included in M^n (see appendix B of [8] for an example of sets and the proof of the following property).

PROPOSITION 5.1 *We set $V_I = u_1$ and $P_I = P_2$ and we consider an ideal gas law (this is also available for stiffened gas equations of state). Let $\overline{u_1}$ be a real constant, $\overline{P_2} > 0$ and $p_0 \geq 0$ be constants.*

We assume that Δt^n is small enough to ensure the positivity of the different variables which have to be.

If at time $t = 0$ these conditions hold:

$$(P_2)_K^0 = \overline{P_2} \in \mathbb{R} \;\; (P_1)_K^0 = \frac{p_0}{(\alpha_1)_K^0} + \overline{P_2} \quad \forall K \in M^0$$

$$\text{and } (u_1)_{K'}^0 = (u_2)_{K'}^0 = \overline{u_1} \in \mathbb{R} \quad \forall K' \in M^0 (\text{ resp. } K' \in M_D^0)$$

then the discretization obtained after n time iterations using the Rusanov scheme (resp. BN_SSIEE scheme) verifies:

$$(P_2)_K^n = \overline{P_2} \quad (P_1)_K^n = \frac{p_0}{(\alpha_1)_K^n} + \overline{P_2} \qquad \forall K \in M^n$$

$$(u_1)_{K'}^n = (u_2)_{K'}^n = \overline{u_1} \text{ on each cell } K' \text{ of } M^n \text{ (resp. } M_D^n)$$

This result means that the velocities and the interfacial pressure are exactly resolved for type-2 solutions with the Rusanov scheme and BN_SSIEE, and that the relation between α_1 and P_1 is maintained. This result is also useful for some kinds of contact discontinuities (see section 5.2.1).

The four numerical schemes have been tested on a type-2 smooth solution. We consider the space domain $[0; 1]$. The final time is $T_f = 0.01$. The EOS parameters are $\gamma_1 = 2$ and $\gamma_2 = 3$. Initial conditions are as follows:

$$\alpha_2(x,0) = 0.98/(0.5 * 0.2 - 0.5 * 0.4)^6 * (x - 0.2)^3 * (x - 0.4)^3 \mathbf{1}_{[0.2;0.4]} + 0.99$$
$$m_1(x,0) = (x - 0.3)^5 * (x - 0.5)^5 \mathbf{1}_{[0.3;0.5]} + 0.01$$
$$m_2(x,0) = (x - 0.15)^4 * (x - 0.45)^4 \mathbf{1}_{[0.15;0.45]} + 0.99$$

$$P_2(x,0) = 0.5 \qquad P_1(x,0) = \frac{0.5}{1 - \alpha_2(x)} + P_2(x,0)$$
$$u_1(x,0) = u_2(0,t) = 0.8$$

For all the simulations the CFL number is equal to 0.5.

Figure 2 shows the results obtained with the four schemes using a 500 cells mesh. The Rusanov and BN_SSIEE schemes maintain u_1, u_2 and P_2 constant as expected. The relaxation scheme maintains these variables nearly constant too: the errors obtained seem to vanish when ϵ tends to 0 (see figure 1). The VFROE-ncv produces some oscillations on these variables. We note that the Rusanov scheme is very dissipative on the other variables with respect to the other schemes. Moreover the behavior of ρ_2 is wrongly evaluated. VFROE-ncv, BN_SSIEE and the relaxation scheme have a close behavior on α_2, ρ_1, ρ_2 and P_1.

Figure 3 shows the convergence of the schemes. As regards u_1, u_2 and P_2, only the error obtained with VFROE-ncv is drawn; the meshes are not refined enough to get the theoretical asymptotic rate of convergence. As regards the other variables the errors obtained for the relaxation scheme, VFROE-ncv and BN_SSIEE are

approximately equal independently of the mesh size and the four schemes seem to converge, with a h^1 asymptotic rate of convergence.

The measured CPU times are now considered as a function of the errors (figure 4). We note some major differences among the schemes. The runtime of BN_SSIEE scheme is low (table 1). This can be explained by the fact that no expensive calculations (root calculations for instance) must be made, except for the time step obtained using the CFL condition (2). The long CPU time of the relaxation scheme is due to some implicit resolutions and the high one of the VFROE-ncv scheme is related to the considerable number of root calculations. The Rusanov scheme has a low CPU cost if considered as a function of the mesh size, but is the most expensive if considered as a function of the error.

Table 1: Test 1 - Measured CPU times for the 200,000 cells mesh (seconds)

	Rusanov	Relaxation	BN_SSIEE	VFROE-ncv
CPU time	3311 s	32256 s	3948 s	103678 s

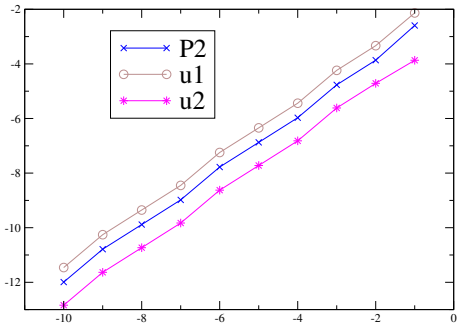

Figure 1: Test 1 - Relaxation scheme - 1,000 cells - $\log_{10}$ of the error with L^1 norm as a function of $\log_{10}(\epsilon)$

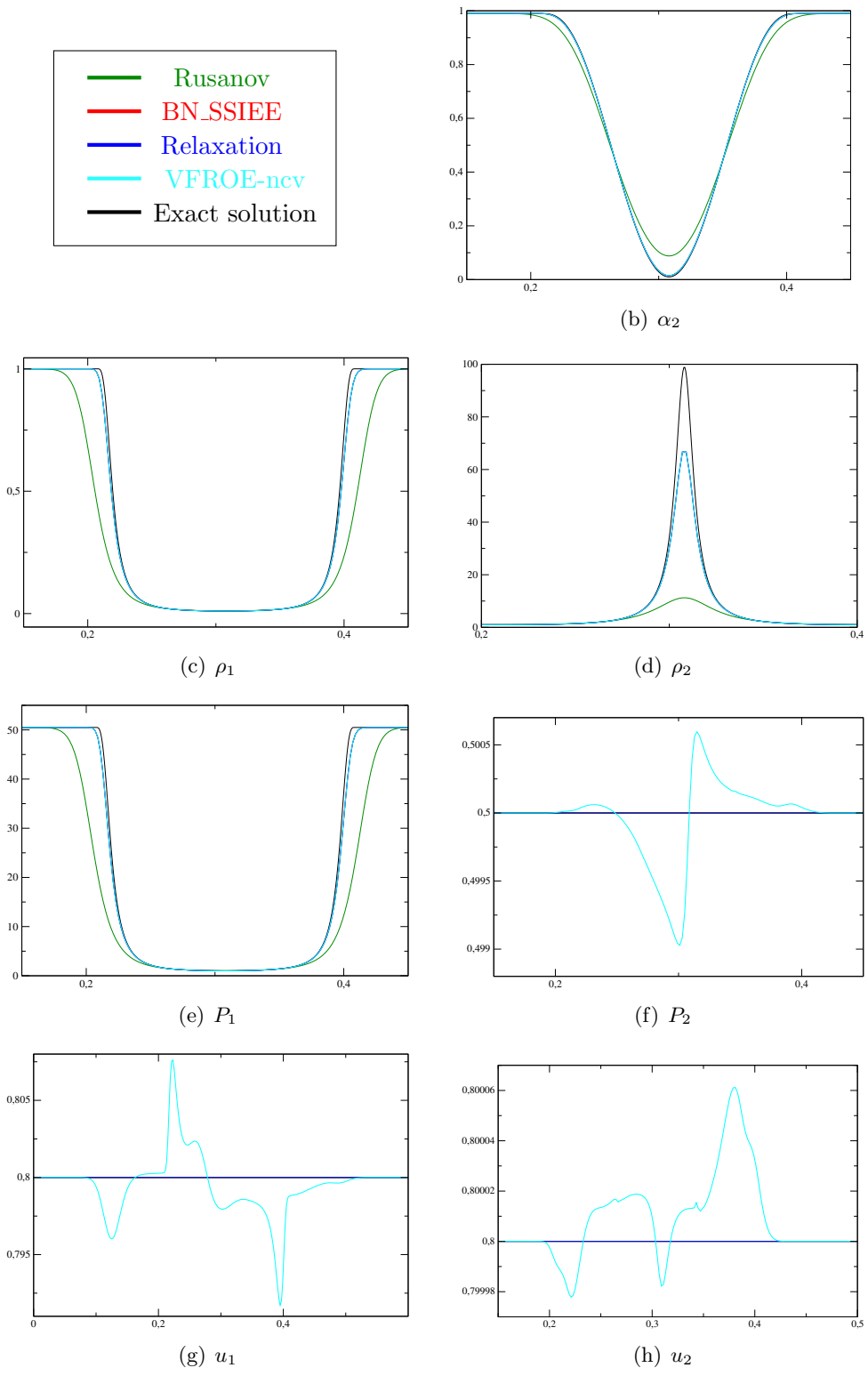

(b) α_2

(c) ρ_1

(d) ρ_2

(e) P_1

(f) P_2

(g) u_1

(h) u_2

Figure 2: Test 1 - Results for 500 cells

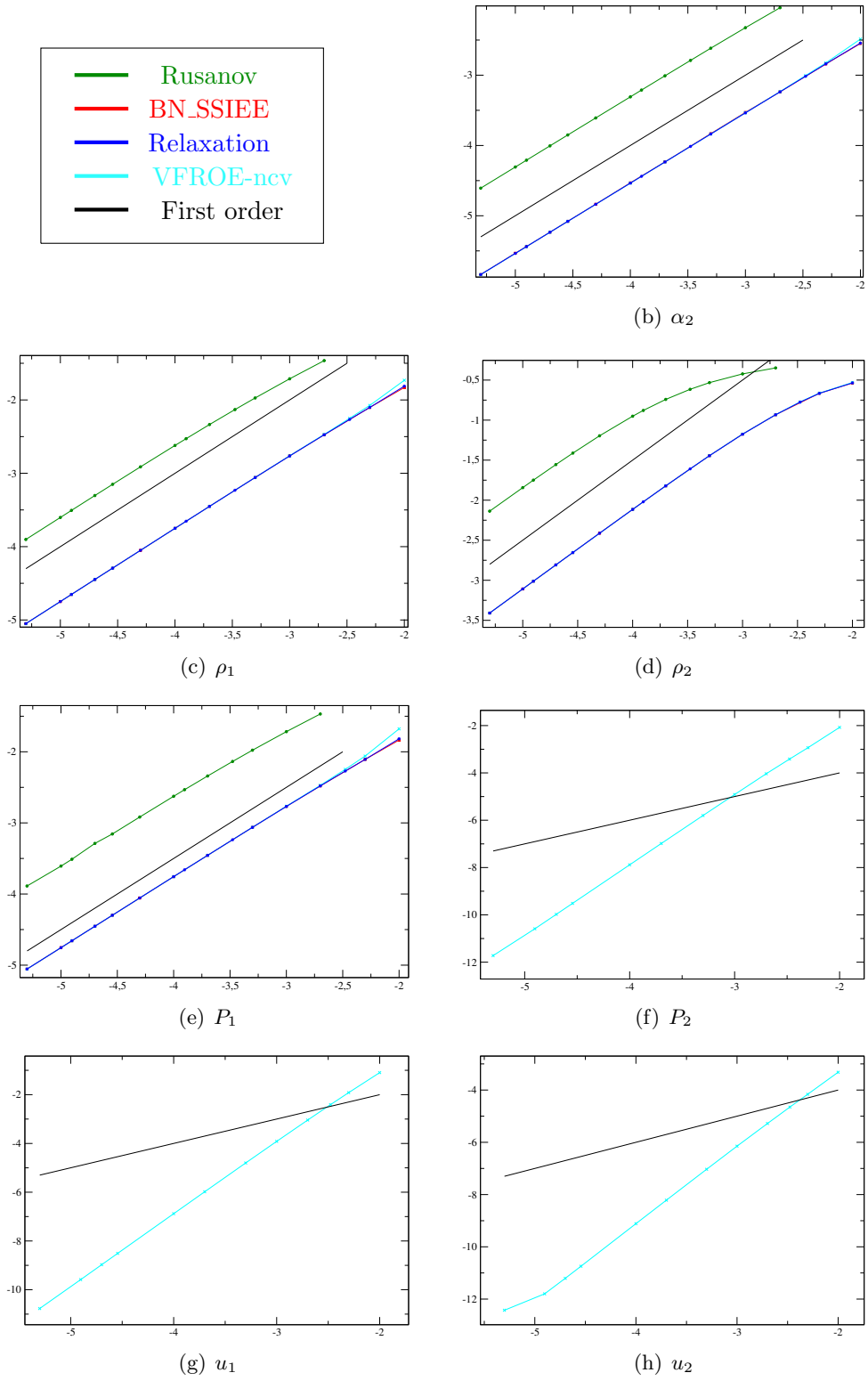

(b) α_2

(c) ρ_1

(d) ρ_2

(e) P_1

(f) P_2

(g) u_1

(h) u_2

Figure 3: Test 1 - $\log_{10}$ of the L^1 norm of the error as a function of $\log_{10}(h)$

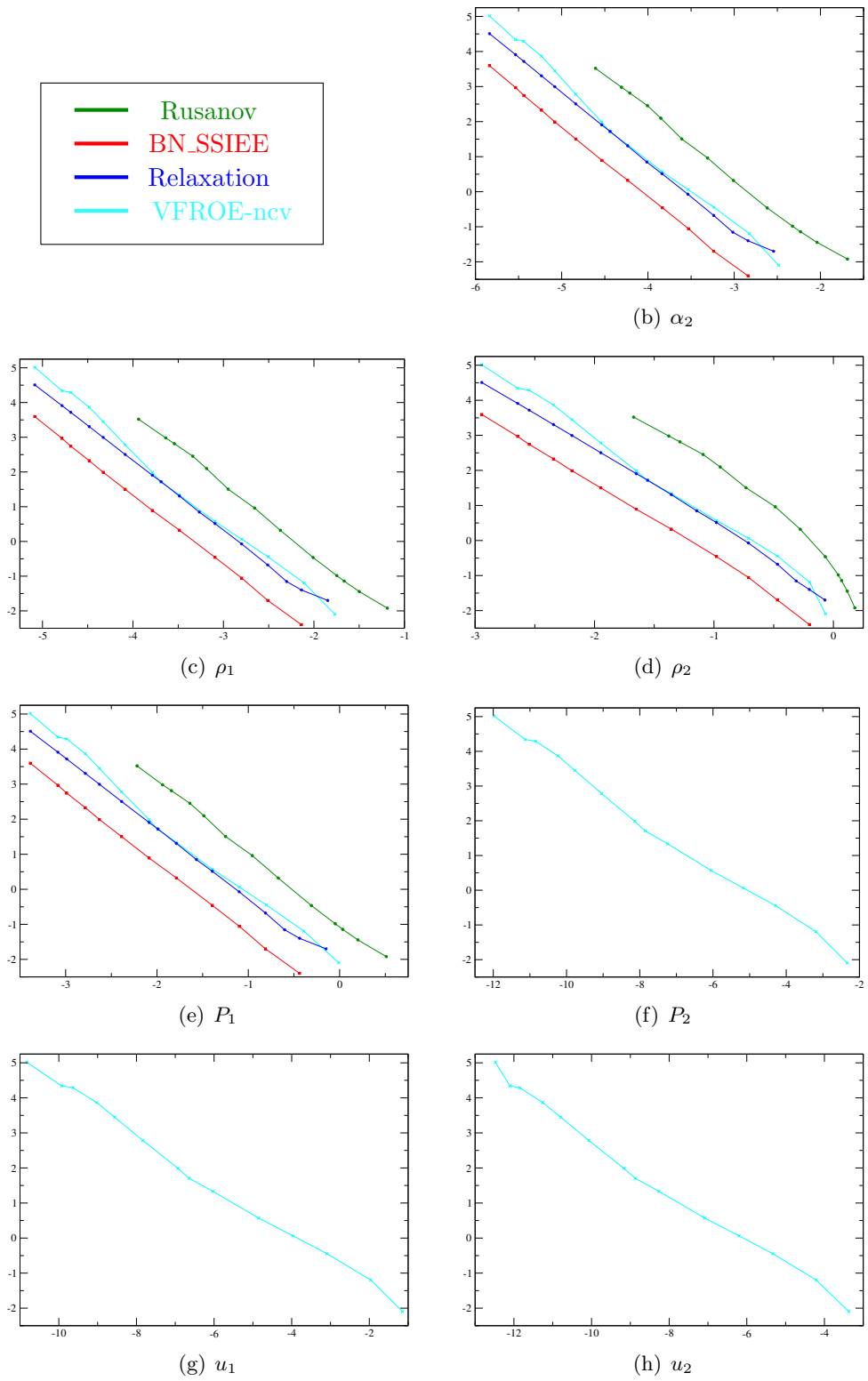

(b) α_2 (c) ρ_1 (d) ρ_2 (e) P_1 (f) P_2 (g) u_1 (h) u_2

Figure 4: Test 1 - $\log_{10}$ of CPU time as a function of $\log_{10}$ of the error with L^1 norm

5.1.2 Test 2: Isolated coupling wave

The solution of this first Riemann problem is a contact discontinuity associated with V_I with a reasonable jump of α_k. Initial conditions have been chosen such that velocities are not equal and such that interfacial pressure P_I is discontinuous, in order not to have a specific contact (see test 1 and test 4) for which most numerical schemes have a very good behavior due to those very specific initial conditions.

Table 2: Test 2 - model and simulation parameters

V_I	P_I	γ_1	γ_2	Domain	X_{disc}	T_f	CFL
u_1	P_2	2	3	$[0;1]$	0.5	0.1	0.5

Table 3: Test 2 - inital conditions

	α_2	ρ_1	ρ_2	u_1	u_2	P_1	P_2
Left state	0.2	1.5185185	1.25	0.3110988	0.1837722	1.2	1
Right state	0.8	0.5	1.2539534	0.3110988	0.2793675	1.7771419	1.0095183

Even though all the four tested schemes converge (see figure 6), with a $h^{\frac{1}{2}}$ asymptotic rate of convergence as expected, we note that this kind of solution is wrongly estimated by numerical schemes in a general way: a considerable error is produced on coarse meshes.

Several kinds of behavior are observed among tested schemes. The results obtained with a 1,000 cells mesh are shown in figure 5. The schemes produce some oscillations located at the position of ghost waves $u_k \pm c_k$ (see [2] for another example). The oscillations are considerable with the BN_SSIEE scheme, in particular for the variables ρ_2, u_1 and P_2. Those obtained with VFROE-ncv make the results not very accurate when coarse meshes are used, but they narrow rapidly during mesh refinement. The results obtained for α_2, ρ_1 and P_1 with BN_SSIEE, VFROE-ncv and the relaxation scheme are very close. The Rusanov scheme is very dissipative. The relaxation scheme has a very good behavior and accuracy.

The errors obtained with the relaxation scheme, BN_SSIEE and VFROE-ncv are close for α_2, ρ_1 and P_1 independently of the mesh size (see figure 6). If the error is taken as fixed for one of these variables, then the BN_SSIEE scheme thus needs a lower run time than the other schemes to reach this error (figure 7) while VFROE-ncv and the relaxation scheme need the same order of magnitude of run time (VFROE-ncv is a little better than the relaxation scheme on fine meshes and

a little worse on coarse meshes). In spite of a low run time with respect to the size of the mesh, the Rusanov scheme is the slowest for a fixed error because of its dissipative behavior. We now focus on ρ_2, P_2 and u_1. The accuracy of the BN_SSIEE scheme is poor, as regards fixed mesh size or even fixed CPU time, due to the oscillations near the ghost waves. However adding some other waves in the Riemann problem radically increases the accuracy (see section 5.1.3) compared to the other schemes. The VFROE-ncv scheme is not very accurate, in particular with coarse meshes, but converges in practice faster than expected until reaching the asymptotic rate of convergence. Lastly, as regards u_2 the most accurate scheme for a fixed mesh size is the relaxation one while the most accurate for a fixed CPU time is BN_SSIEE.

Table 4: Test 2 - Measured CPU times, simulations with 200,000 cells (seconds)

	Rusanov	Relaxation	BN_SSIEE	VFROE-ncv
CPU time	6449 s	43425 s	7043 s	36768 s

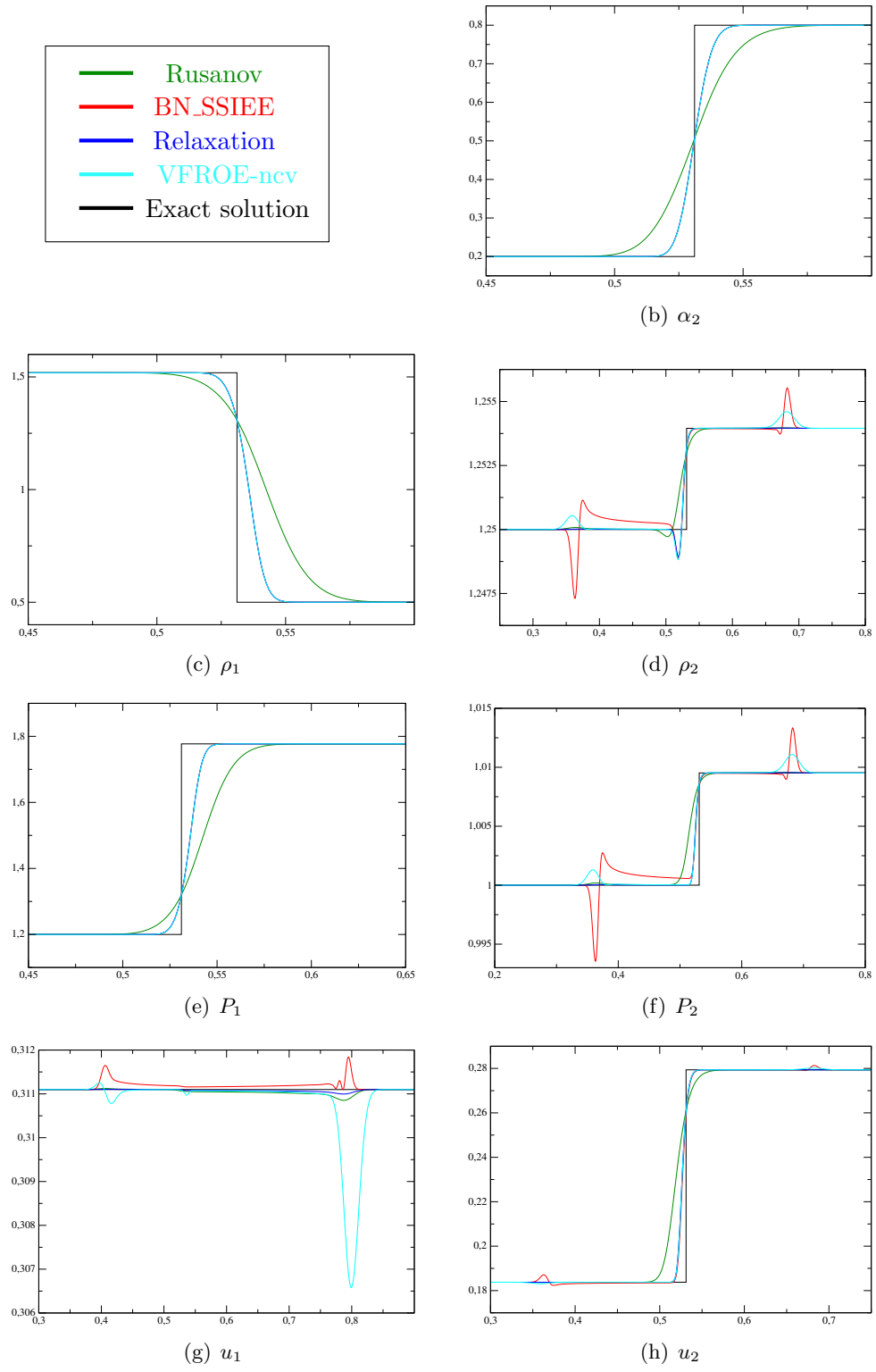

(b) α_2

(c) ρ_1

(d) ρ_2

(e) P_1

(f) P_2

(g) u_1

(h) u_2

Figure 5: Test 2 - results with a 1000-cells mesh

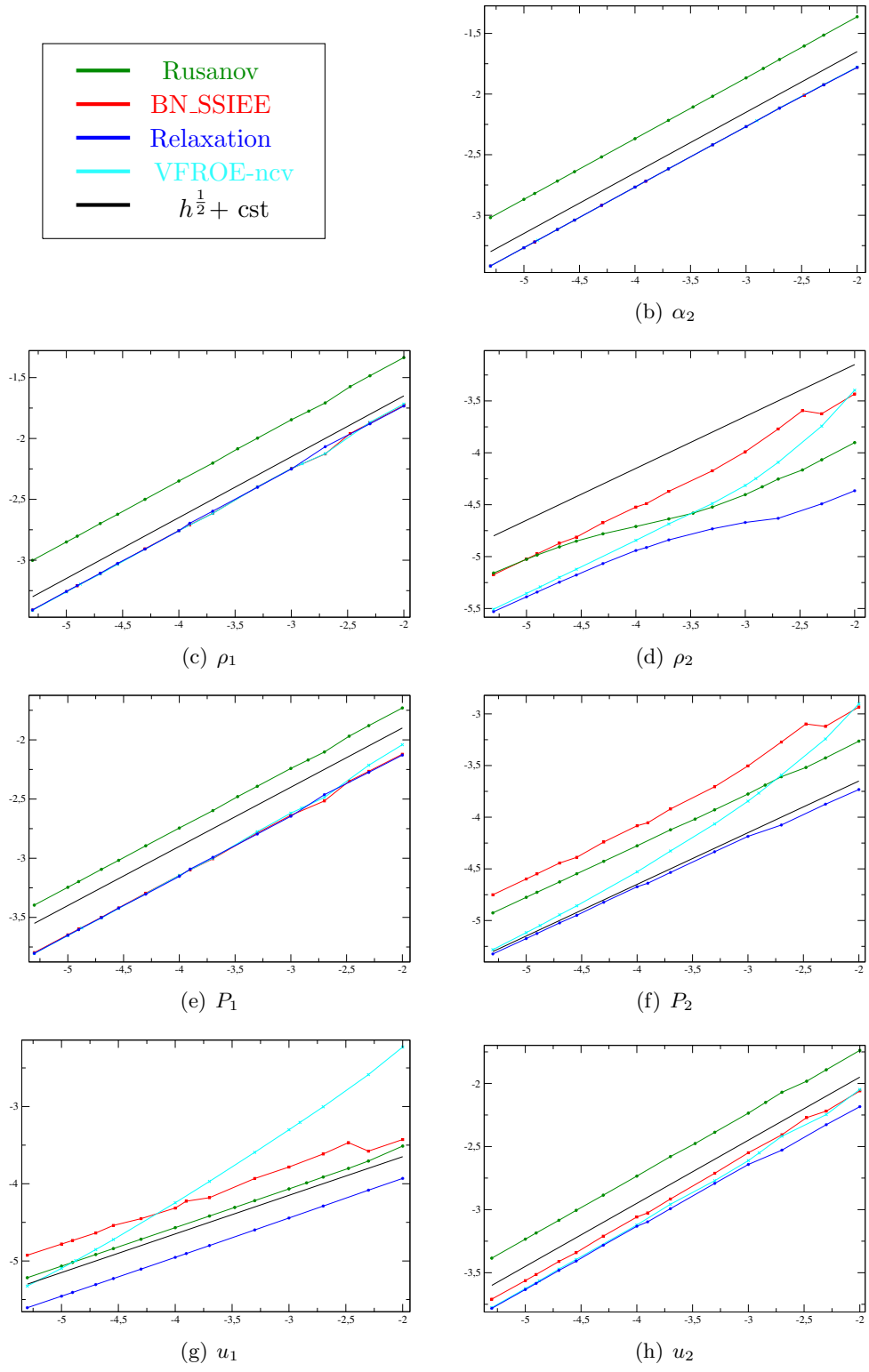

(b) α_2

(c) ρ_1

(d) ρ_2

(e) P_1

(f) P_2

(g) u_1

(h) u_2

Figure 6: Test 2 - $\log_{10}$ of the L^1 norm of the error as a function of $\log_{10}(h)$

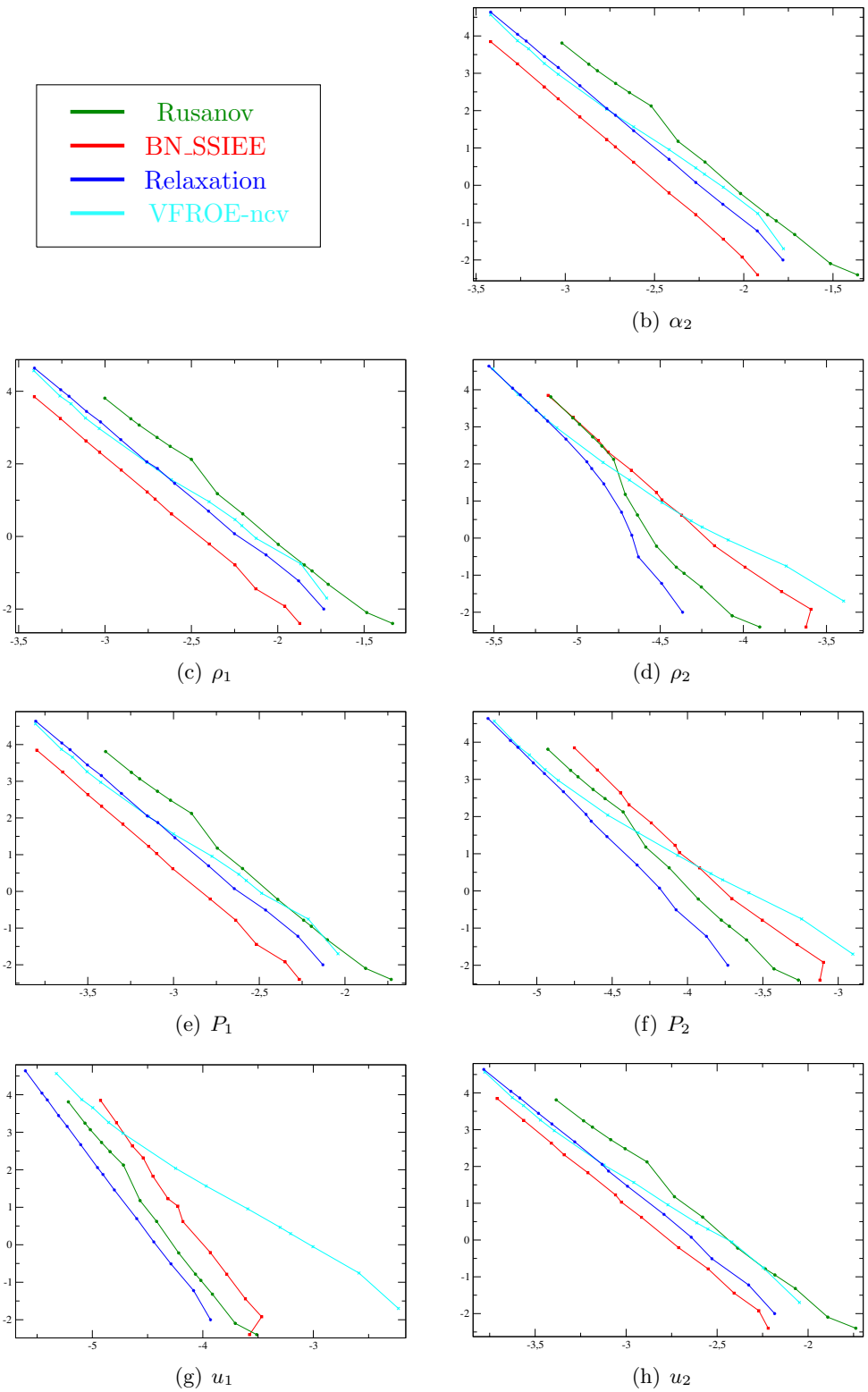

(b) α_2

(c) ρ_1

(d) ρ_2

(e) P_1

(f) P_2

(g) u_1

(h) u_2

Figure 7: Test 2 - $\log_{10}$ of CPU time as a function of $\log_{10}$ of the error with L^1 norm

5.1.3 Test 3: Coupling wave and shock waves

The following test is a Riemann problem. The solution is made of two shock waves and one contact discontinuity (the one associated with V_I). The constant states of the solution are given in table 6. The contact discontinuity separates the same states as the ones considered in the previous test.

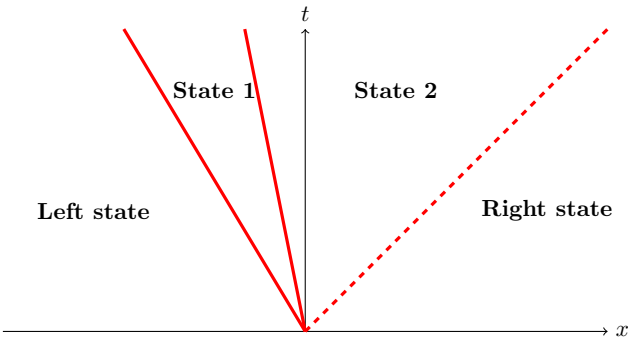

Figure 8: Test 3 - Pattern of the solution

Table 5: Test 3 - model and simulation parameters

V_I	P_I	γ_1	γ_2	Domain	X_{disc}	T_f	CFL
u_1	P_2	2	3	$[0;1]$	0.5	0.1	0.5

Table 6: Initial and intermediary states of test 3

State	α_2	ρ_1	ρ_2	u_1	u_2	P_1	P_2
Left	0.2	1	1	0.8	0.5	0.5	0.5
1	0.2	1	1.25	0.8	0.1837722	0.5	1
2	0.2	1.5185185	1.25	0.3110988	0.1837722	1.2	1
Right	0.8	0.5	1.2539534	0.3110988	0.2793675	1.7771419	1.0095183

The results obtained with 100 cells are shown on figure 9. As in the previous test, BN_SSIEE produces oscillations near the ghost waves $u_1 + c_1$ and $u_2 + c_2$. The relaxation scheme and VFROE-ncv have a similar behavior except near the ghost waves and for ρ_2 where the relaxation scheme is more accurate. The BN_SSIEE scheme is overall more accurate in the neighborhood of the shock waves, using L^1 norm, but is not always monotone. As usual, the Rusanov scheme is very dissipative.

The errors obtained on meshes of 100 to 200,000 cells are drawn on figure 10.

The errors obtained with VFROE-ncv and the relaxation scheme are very close. The curves of BN_SSIEE, VFROE-ncv and the relaxation scheme for α_2 and ρ_1 superimpose. As regards ρ_2, P_2 and u_2 with the BN_SSIEE scheme, the curves of convergence are irregular. Errors obtained are lower between 100 to 10,000 cells and higher with 50,000 and more cells than the ones obtained with VFROE-ncv and the relaxation scheme.

CPU times as a function of the errors are considered on figure 11. In general, the BN_SSIEE scheme is by far the fastest scheme tested with a fixed error, despite the presence of two ghost waves. This is due to the cheap CPU cost with a fixed size mesh and to the accuracy near shock waves. VFROE-ncv is efficient on fine meshes but is not on coarse meshes. The Rusanov scheme is in general less efficient, except for ρ_2 and P_2. Cost estimates for each scheme for a fixed error are given in table 8.

Table 7: Test 3 - Measured CPU times, simulations with 200,000 cells (seconds)

	Rusanov	Relaxation	BN_SSIEE	VFROE-ncv
CPU time	7079 s	43490 s	7171 s	29776 s

Table 8: Test 3 - Estimation of CPU time requisite (seconds) to reach a fixed error (normalized)

	Er(α_2)= 10^{-3}	Er(ρ_1)= $5*10^{-3}$	Er(ρ_2)= $5*10^{-4}$	Er(P_1)= 10^{-3}	Er(P_2)= 10^{-4}	Er(u_1)= 10^{-4}	Er(u_2)= $5*10^{-4}$
Rusanov	5910	30.5	1.25	533.9	291.2	547	881.4
Relaxation	923	6.5	1.84	95.7	297.0	160.5	268.2
BN_SSIEE	134	0.9	0.05	15.3	73.6	50.1	39.9
VFROE-ncv	634	12.9	5.18	99.8	245.5	162.6	232.3

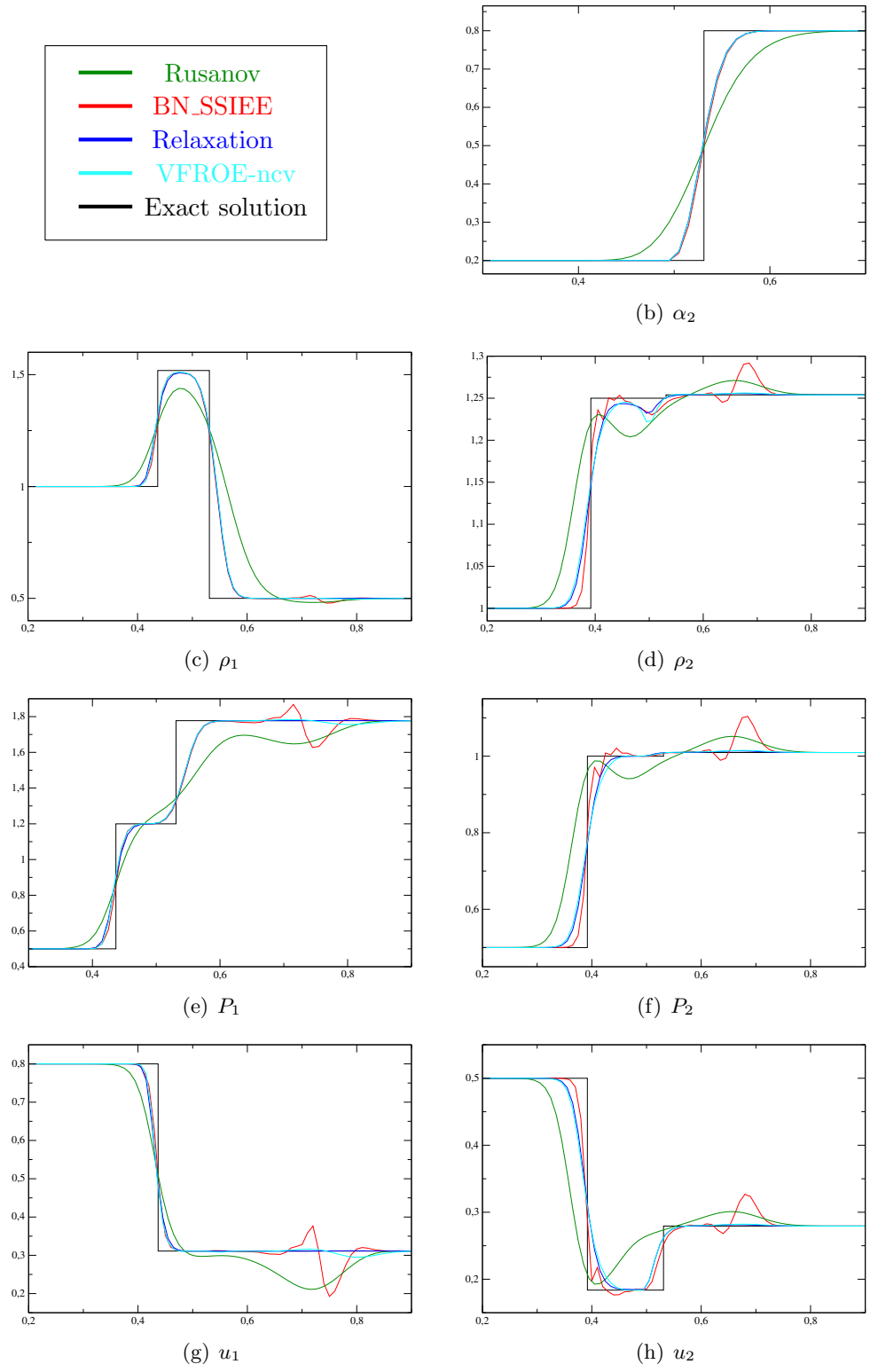

(b) α_2

(c) ρ_1

(d) ρ_2

(e) P_1

(f) P_2

(g) u_1

(h) u_2

Figure 9: Test 3 - Results with 100 cells

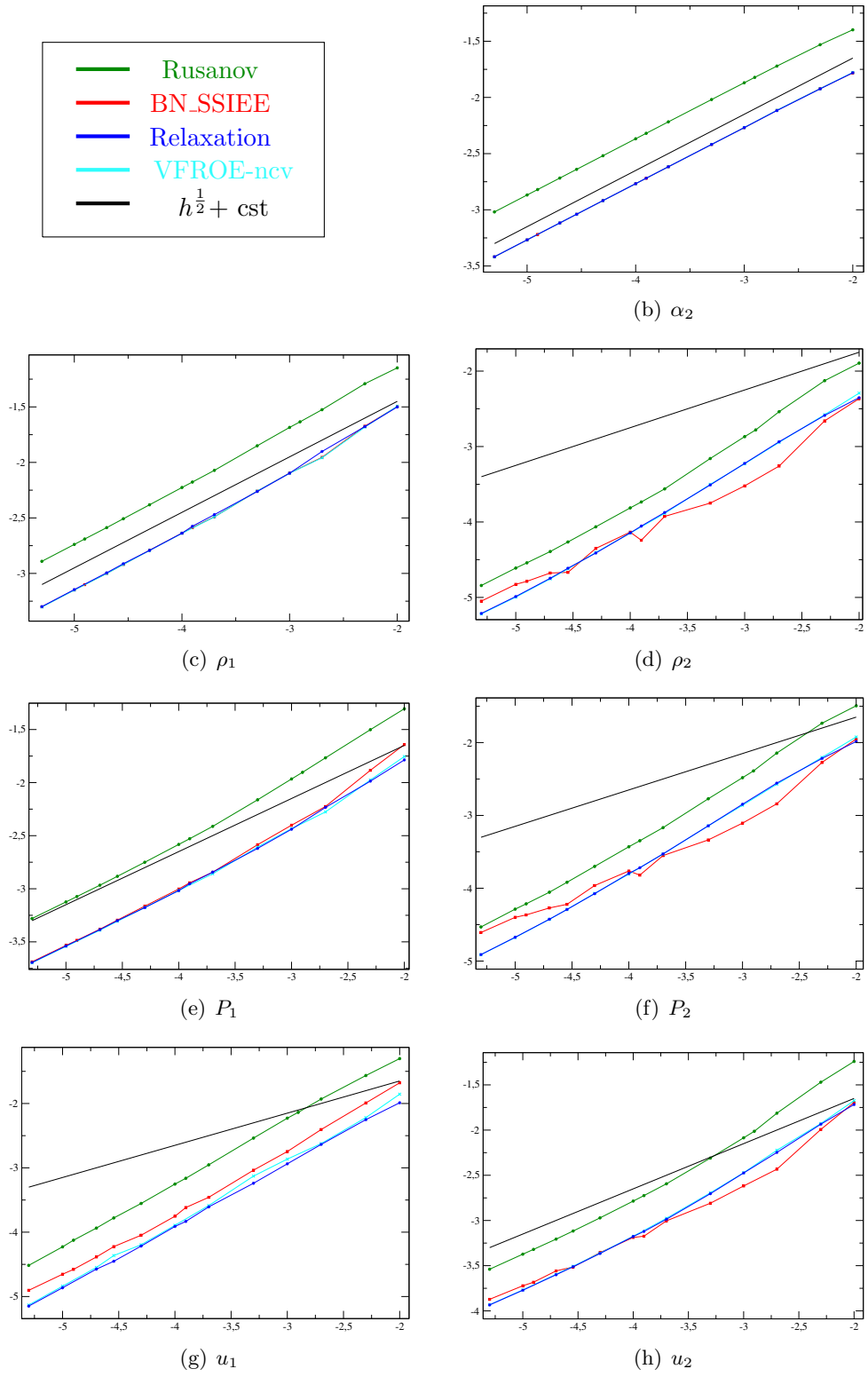

(b) α_2

(c) ρ_1

(d) ρ_2

(e) P_1

(f) P_2

(g) u_1

(h) u_2

Figure 10: Test 3 - $\log_{10}$ of the L^1 norm of the error as a function of $\log_{10}(h)$

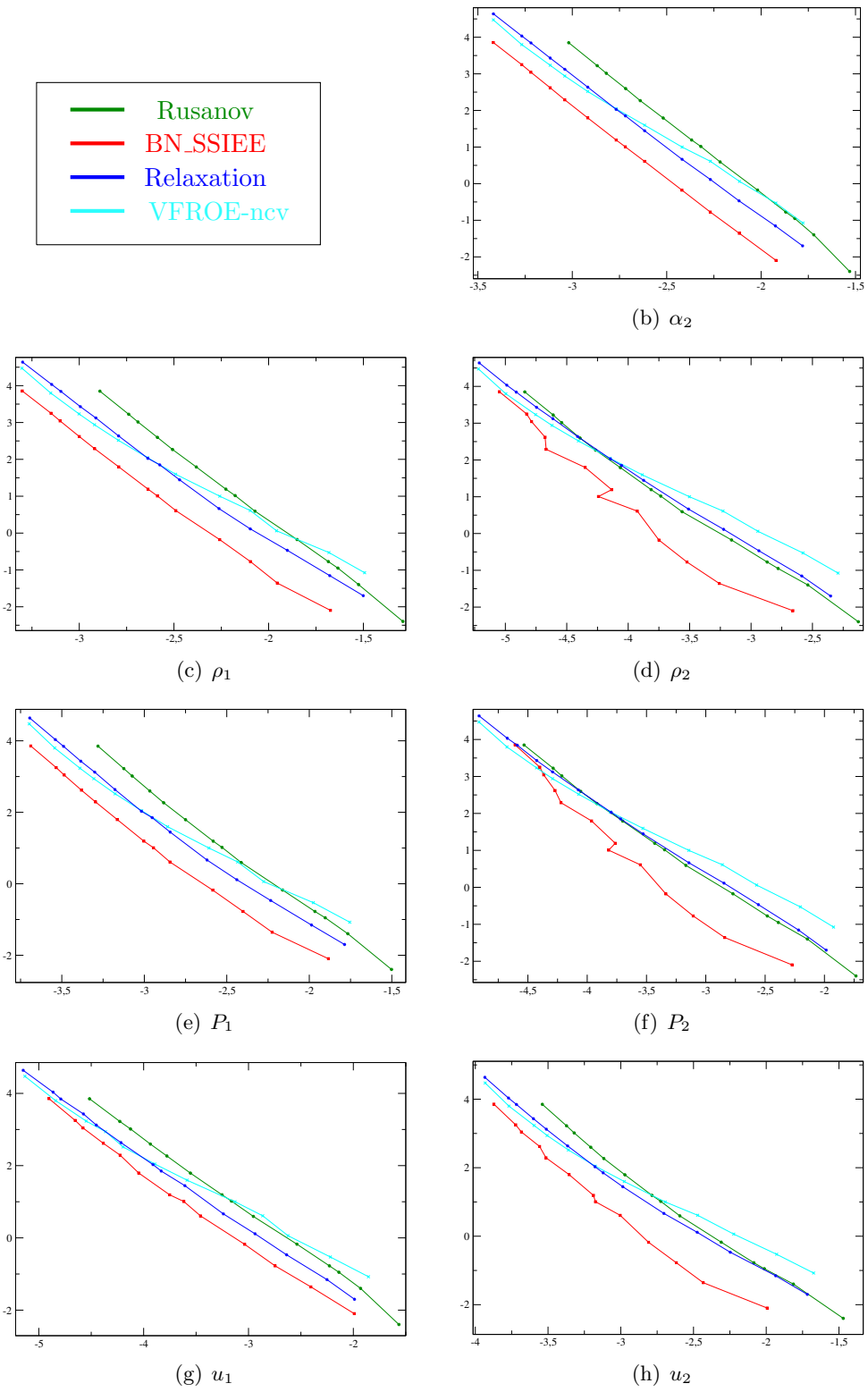

(b) α_2

(c) ρ_1

(d) ρ_2

(e) P_1

(f) P_2

(g) u_1

(h) u_2

Figure 11: Test 3 - $\log_{10}$ of CPU time as a function of $\log_{10}$ of the error with L^1 norm

5.2 Stiffened gas - Ideal gas

In this section, the equations of state are the following:

$$P_k = (\gamma_k - 1)\rho_k e_k - \gamma_k P_{k,0} \qquad \text{with } \gamma_k > 1$$

and with $P_{k,0} = 0$ for one of the phases and $P_{k,0} > 0$ for the other one.

5.2.1 Test 4: A stationary isolated coupling wave

The solution considered in this test is a stationary isolated contact wave taken from [25]. The final time T_f is chosen shorter than in the original test, because of the dissipative behavior of the Rusanov scheme. This kind of contact wave is generally well approximated by the schemes, because $u_1 = u_2 = 0$ and P_I is constant across the contact discontinuity associated with V_I. We establish the following proposition:

PROPOSITION 5.2 *Stiffened gas or ideal gas equations of state are considered. A Riemann problem is considered where the solution W_{exact} is made of constant states separated by a V_I-contact discontinuity such that the initial state verifies:*

$$(u_1)_L = (u_1)_R = (u_2)_L = (u_2)_R = 0 \quad \textit{and} \quad (P_I)_L = (P_I)_R$$

Let W_K^n be the approximate solution obtained on a primal cell K at the n^{th} time iteration using the BN_SSIEE scheme (we assume that the discretizations of the volume fractions, the densities and the square of the sound velocities remain positive).

Then for all cell K in M^n: $\quad W_K^n = W_{exact}(x_K, t^n)$

where M^n is defined section 5.1.1 and x_k is the center of the cell K.

The proof of this proposition is available in an appendix of [8].

Remark 2 This property is verified by a lot of schemes and is due to these specific initial conditions.

Remark 3 We have shown (proposition 5.1) that the Rusanov scheme resolves exactly the constant states u_1, u_2 and P_I for this kind of problem. It should be emphasized that the interfacial pressure P_I may be discontinuous across a stationary contact discontinuity associated with V_I, and in this case the velocities are no longer resolved exactly by the Rusanov scheme.

Table 9: Test 4 - model and simulation parameters

V_I	P_I	γ_1	$P_{1,0}$	γ_2	$P_{2,0}$	Domain	X_{disc}	T_f	CFL
u_2	P_1	1.4	0	3	10	$[0;1]$	0.5	0.05	0.9

Table 10: Test 4 - inital conditions

	α_2	ρ_1	ρ_2	u_1	u_2	P_1	P_2
Left	0.6	1.4	1.4	0	0	1	2
Right	0.3	1	1	0	0	1	3

The results obtained with 100 cells are shown in figure 12. The BN_SSIEE scheme resolves exactly the solution as expected. These results are not visible because they coincide with those obtained with the relaxation scheme. The Rusanov scheme, except for u_1, u_2 and P_1, does not resolve the solution exactly; this is due to the dissipative term added to ensure the stability.

Some oscillations occur on the constant states with VFROE-ncv. However these oscillations don't seem to hinder the convergence when the mesh is refined. We note that other results may be obtained for VFROE-ncv; this is due to the choice of the approximate value at the interface between two cells: indeed, if at least one eigenvalue of the approximate linearized set of equations is equal to zero then the interfacial states are undefined (see appendix A of [8]). If $Q^* = Q_L + \sum_{j|\lambda_j \leq 0} \xi_j r_j$ or $Q^* = Q_L + \sum_{j|\lambda_j < 0} \xi_j r_j$ or any linear combination of these terms is chosen then oscillations will occur: in any case V_I^* is not equal to zero (near the initial location of the discontinuity) since the first time iteration.

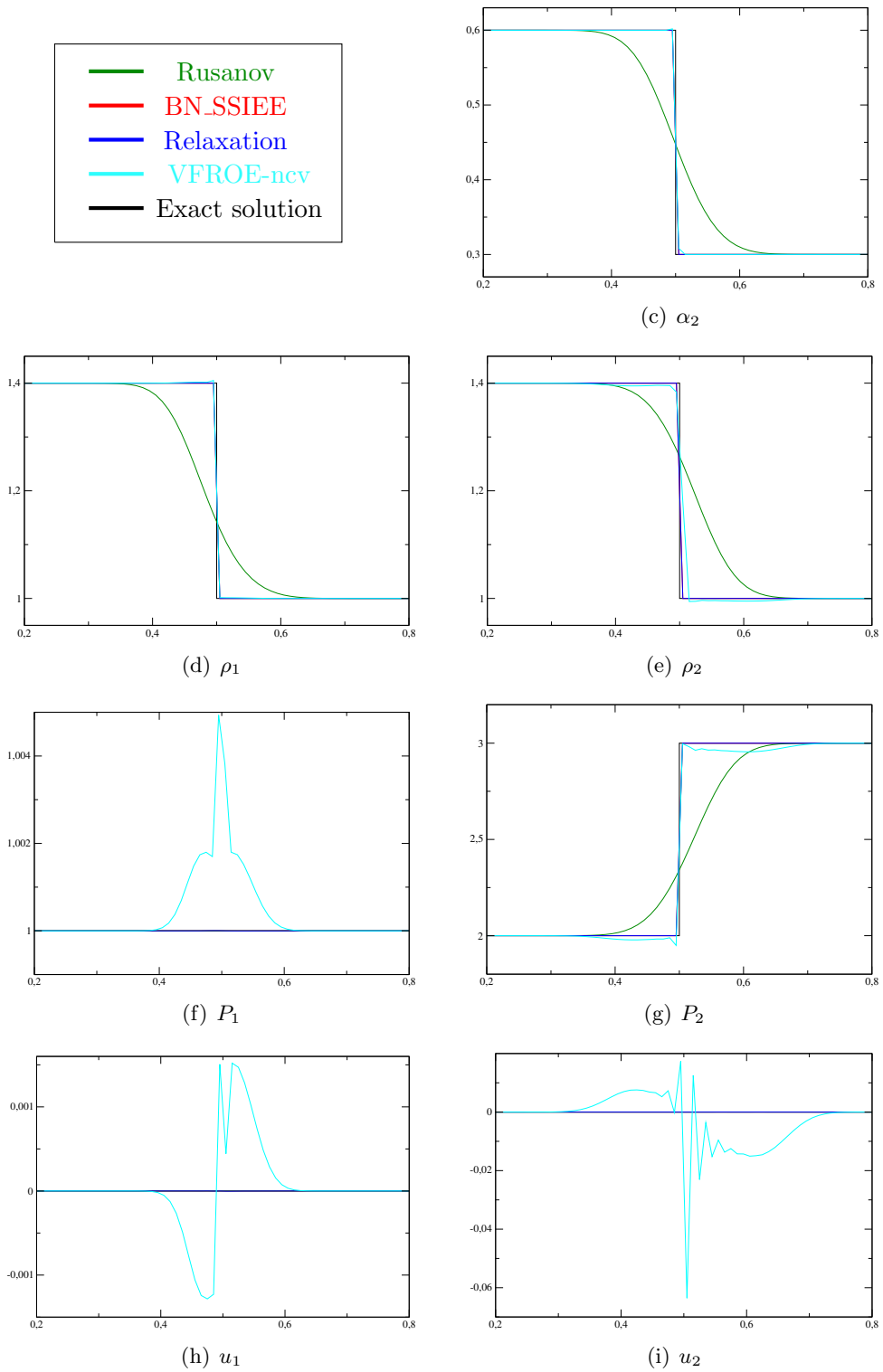

(c) α_2

(d) ρ_1

(e) ρ_2

(f) P_1

(g) P_2

(h) u_1

(i) u_2

Figure 12: Test 4 - results obtained with 100 cells

5.2.2 Test 5: A general Riemann problem

This test is taken from [25]. Phase 1 has an ideal gas equation of state while phase 2 has a stiffened gas one. The exact solution is composed of two rarefaction waves, one contact discontinuity and two strong shock waves.

Table 11: Test 5 - model and simulation parameters

V_I	P_I	γ_1	$P_{1,0}$	γ_2	$P_{2,0}$	Domain	X_{disc}	T_f	CFL
u_2	P_1	1.4	0	3	100	$[0;1]$	0.8	0.007	0.9

Table 12: Test 5 - inital conditions

	α_2	ρ_1	ρ_2	u_1	u_2	P_1	P_2
Left	0.7	1	1	-19.5975	-19.5975	1000	1000
Right	0.2	1	1	-19.5975	-19.5975	0.01	0.01

We note that the Mach number $Ma = \frac{|u_1|}{\sqrt{\gamma_1 P_1/\rho_1}}$ of phase 1 is initially approximately equal to 0.52 at the left and to 165.6 at the right. In applications, we most often consider subsonic flows (ie $Ma < 1$); however this case is interesting to assess the behavior of the algorithms on strong shock waves.

Regarding VFROE-ncv a loss of positivy on ρ_1 occurs at the first time iteration. This trouble is due to the strong jump of pressure P_1: the approximate entropy at the interface between left and right states is very small (0.01) because of the simple upwinding of the entropy, whereas the pressure at the interface P_1^* (500.005) is obtained using left and right pressures. Consequently, the density at the interface ρ_1^* is very large (approximately 2272), hence the positivity is lost. We note that this problem does not occur on phase 2 despite the same initial jump of pressure and partial mass because of the use of a different equation of state: thanks to $P_{2,0}$ the entropy at the interface (100.01) is higher than the one of phase 1. The same test has been carried out by increasing the CFL number slowly, and then with a very small fixed CFL number ($9 * 10^{-9}$), but that turned out to be insufficient. This kind of problem may also occur with the Euler equations.

Figure 13 shows the results obtained with the three other schemes. The Rusanov scheme is very dissipative as usual and has some difficulties to approximate the intermediary states, in particular the peak on ρ_2. The results obtained using BN_SSIEE are better than using Rusanov, but an oscillating behavior is observed on some states. However, these oscillations are reduced when the mesh is refined. The relaxation scheme has good behavior, the results seem to be similar to the ones obtained with HLLC in [25].

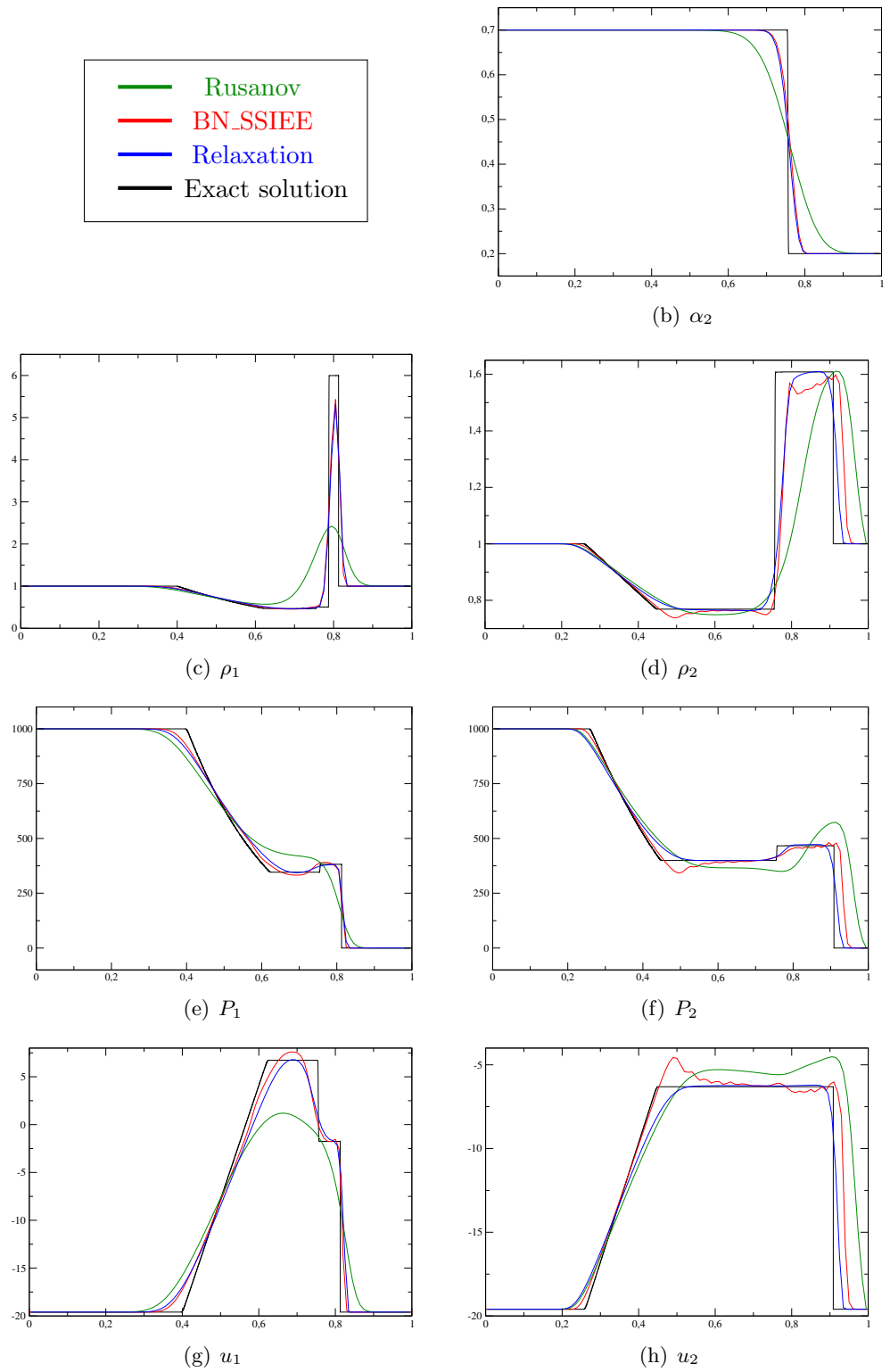

(b) α_2

(c) ρ_1

(d) ρ_2

(e) P_1

(f) P_2

(g) u_1

(h) u_2

Figure 13: Test 5 - Results obtained with 100 cells

6 Summary of the results

A benchmark study has been carried out in order to compare four numerical schemes on the convective and unidimensional part of the Baer-Nunziato model.

- The first test case does not require a lot of robustness and allows the comparison of the accuracy and runtime of the schemes. We observe that the proposed smooth solution verifies the Riemann invariants of a coupling contact discontinuity. An interesting extension should be a solution which verifies those invariants with u_2 not constant in order to get P_2 and α_2 not constant simultaneously. Such a solution coupled with a coupling contact discontinuity should be useful to check the constistency of schemes with non-conservative products.

- The second test case is an isolated coupling discontinuity. This test is important because this kind of wave does not exist in the single phase framework (Euler equations) and the behavior of schemes has been less studied for this kind of wave than the other waves (shock, monophasic contact and rarefaction waves). In a general way, schemes are not accurate for this kind of test.

- The third test uses the previous coupling contact discontinuity with two shock waves. This test allows the comparison of the behavior of the schemes on those waves but also to minimize results of test 2: in practice, it is unlikely a contact wave be isolated.

- Tests 4 and 5 have been taken from literature and allow the comparison of the schemes with stiffened gas EOS. It is important to emphasize that initial conditions of test 4 are particular: velocities are both equal to zero and interfacial pressure is constant across the contact. For these initial conditions, schemes have an excellent behavior but these conceal the main numerical complexities (see test 2). Test 5 is also singular because of a high Mach numbers configuration, which is far from our applications. However, this test is interesting to test robustness of schemes in the presence of strong shock waves.

We note that it would be interesting to carry out the following two test cases to complete this study. A first test would be a one with a very strong jump of void fraction. This kind of test is difficult for the schemes and is rarely shown in literature. A second test would be a low Mach case with values near applications.

As regards numerical schemes, the following observations emerge from the study:

- The Rusanov scheme is the scheme which has the lowest CPU times for a fixed size of mesh, but is also the one which produces the most errors for a fixed size of mesh. The second point is not compensated by the first one, this scheme is not competitive against the three other schemes.

- The BN_SSIEE scheme, which has been explored for reasons related to source terms, in general is not the most accurate for a fixed size of mesh; this is due to a poor accuracy near the ghost waves. However the low CPU time cost seems to compensate the lack of accuracy that may sometimes occur. This scheme - which is a very good scheme in the monophasic case - should be improved in the case of the BN model to be more robust when strong jumps of void fraction are considered and to be more accurate on coupling waves.

- The relaxation scheme appears to be the best candidate from an industrial point of view. Indeed, this scheme is accurate, even on coarse meshes, with an acceptable cost when compressible flows are considered and is robust, in particular when the jump of the void fraction is near 1, a kind of test which has not been shown in this article.

- The accuracy for a fixed size of mesh of the VFROE-ncv scheme is satisfactory but this scheme is quite expensive in terms of CPU time. However, some problems of loss of positivity may occur, in particular when strong jumps of void fractions are considered. In a general way, this scheme does not seem to have benefits with respect to the relaxation scheme.

The results obtained in this study provide information about the behavior, the accuracy and the CPU cost of some convective schemes in the one-dimensional case and provide trends as regards the multidimensional and full BN model. However, the above conclusions must take the following remarks into account. In practice, the relaxation source terms - which are not considered in this article - are handled using splitting methods. The numerical resolution of these terms - on each cell of the mesh - includes implicit methods, the CPU costs of which are significant. If only convection is considered, a scheme may be faster and more accurate using a finer mesh than a scheme which is more accurate for a fixed size of mesh. However, in the case of the full model with source terms, the time step is still computed using the CFL condition of the convective part, so to refine the mesh involves much more implicit calculations. It would be interesting to carry out some tests on the full BN model in order to have an estimation of the runtimes and the errors of the source terms and convective parts.

Acknowledegments

The author benefits from financial support through an EDF-CIFRE contract 2013/0608. The author would like to thank Khaled Saleh who made the code he wrote for the relaxation approach available for this study.

Appendix A: The BN_SSIEE scheme

The BN_SSIEE (Staggered Scheme using Internal Energy Equations for the Baer-Nunziato model) scheme is briefly reminded. More details are given in [7]. The main feature of this scheme is to use the discretization of the internal energy equations (A.1.k) instead of total energy equations (4.k). The equations (A.1.k) may be a substitute for the equations (4.k) in an equivalent manner when smooth solutions are considered, but not in the attendance of (discontinuous) shock waves:

$$\partial_t(m_k e_k) + \partial_x(m_k e_k u_k) + \alpha_k P_k \partial_x(u_k) + u_k P_I \partial_x(\alpha_k) + P_I \partial_t(\alpha_k) = 0 \qquad \text{(A.1.k)}$$

A corrective term is thus used in the discretization of (A.1.k) in order to get a consistant weak discretization of the model (1-4) near the shock wave (see [16]).

A first mesh (primal mesh) is used to discretize (1), (2.k) and (A.1.k) (k=1 or 2), and a second mesh (dual mesh), built using the primal mesh, is used to discretize the momentum balance equations (3.k). In this reminder, regular meshes are used; otherwise the weight of average values of the variables and of the fluxes are not equal to 1/2 anymore but depend on the volume of the cells (see [7]).

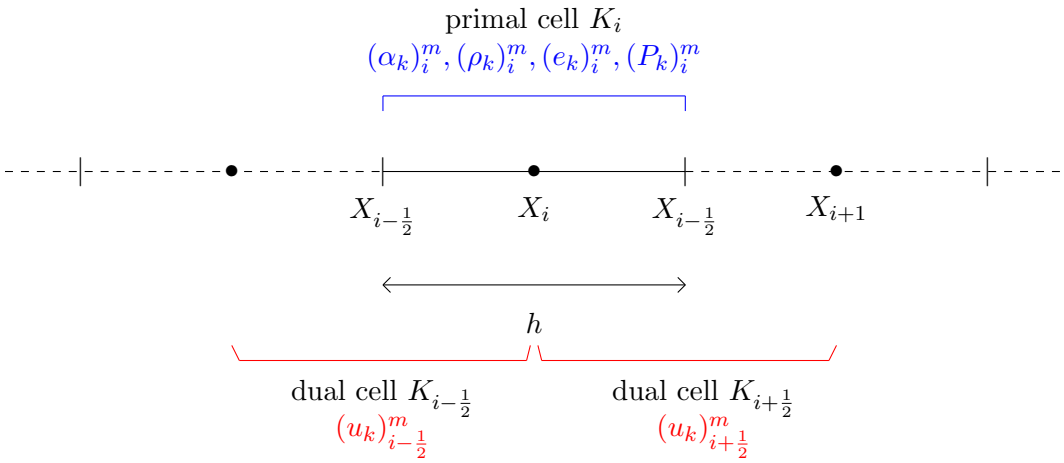

The mass fractions are first determined using the primal mesh:

$$h\frac{\left((\alpha_k\rho_k)_i^{n+1} - (\alpha_k\rho_k)_i^n\right)}{\Delta t} + (F_k)_{i+\frac{1}{2}}^n - (F_k)_{i-\frac{1}{2}}^n = 0 \qquad \text{(A.2.k)}$$

where the numerical fluxes are:

$$(F_k)^n_{i+\frac{1}{2}} = (u_k)^n_{i+\frac{1}{2}} \begin{cases} (\alpha_k\rho_k)^n_i \;\; if \;\; (u_k)^n_{i+\frac{1}{2}} > 0 \\ (\alpha_k\rho_k)^n_{i+1} \;\; otherwise \end{cases}$$

The fraction $(\alpha_2)^{n+1}_i$ is then obtained using the following discretization on the primal mesh:

$$h\frac{\big((\alpha_2)^{n+1}_i - (\alpha_2)^n_i\big)}{\Delta t} \quad + (V_I)^n_{i-\frac{1}{2}}\Big((\alpha_2)^n_i - H^n_{i-\frac{1}{2}}\Big) + (V_I)^n_{i+\frac{1}{2}}\Big(H^n_{i+\frac{1}{2}} - (\alpha_2)^n_i\Big) = 0 \tag{A.3.k}$$

where $(V_I)^n_{i+\frac{1}{2}} = \beta_v(u_1)^n_{i+\frac{1}{2}} + (1-\beta_v)(u_2)^n_{i+\frac{1}{2}}$ (in this article $\beta_v \in \{0;1\}$) and the fluxes $H_{i+\frac{1}{2}}$ are defined by:

$$H^n_{i+\frac{1}{2}} = \begin{cases} (\alpha_2)^n_i \text{ if } (V_I)^n_{i+\frac{1}{2}} > 0 \\ (\alpha_2)^n_{i+1} \text{ otherwise} \end{cases}$$

Internal energy equations (A.1.k) are then discretized using the primal mesh:

$$h\frac{\big((\alpha_k\rho_k e_k)^{n+1}_i - (\alpha_k\rho_k e_k)^n_i\big)}{\Delta t} + (Fe_k)^n_{i+\frac{1}{2}} - (Fe_k)^n_{i-\frac{1}{2}} + (\alpha_k)^n_i(P_k)^n_i\big((u_k)^n_{i+\frac{1}{2}} - (u_k)^n_{i-\frac{1}{2}}\big)$$

$$+(-1)^k(P_I)^n_i\Big[\big((u_k)^n_{i-\frac{1}{2}} - (V_I)^n_{i-\frac{1}{2}}\big)\big((\alpha_2)^n_i - H^n_{i-\frac{1}{2}}\big) + \big((u_k)^n_{i+\frac{1}{2}} - (V_I)^n_{i+\frac{1}{2}}\big)\big(H^n_{i+\frac{1}{2}} - (\alpha_2)^n_i\big)\Big]$$

$$= (S_k)^{n-1}_i \tag{A.4.k}$$

$$\text{where} \qquad (Fe_k)^n_{i+\frac{1}{2}} = (F_k)^n_{i+\frac{1}{2}} \begin{cases} (e_k)^n_i \;\; if \;\; (F_k)^n_{i+\frac{1}{2}} > 0 \\ (e_k)^n_{i+1} \;\; otherwise \end{cases}$$

The corrective terms $(S_k)^{n-1}_i$ on the right handside of the discretization of internal energy equations enable to recover weak total energy balances. They are defined as follows:

$$(S_k)_i^n = \left\| \begin{array}{l} \dfrac{h}{4\Delta t}(m_k)_i^{n+1}\Big[\big((u_k)_{i+\frac{1}{2}}^{n+1} - (u_k)_{i+\frac{1}{2}}^{n}\big)^2 + \big((u_k)_{i-\frac{1}{2}}^{n+1} - (u_k)_{i-\frac{1}{2}}^{n}\big)^2\Big] \\ \\ +\dfrac{1}{2}|(F_k)_i^n|\big((u_k)_{i+\frac{1}{2}}^{n} - (u_k)_{i-\frac{1}{2}}^{n}\big)^2 \\ +(F_k)_i^n\big((u_k)_{i+\frac{1}{2}}^{n} - (u_k)_{i-\frac{1}{2}}^{n}\big) \begin{cases} \big((u_k)_{i+\frac{1}{2}}^{n+1} - (u_k)_{i+\frac{1}{2}}^{n}\big) \text{ if } (F_k)_i^n > 0 \\ \big((u_k)_{i-\frac{1}{2}}^{n+1} - (u_k)_{i-\frac{1}{2}}^{n}\big) \text{ otherwise} \end{cases} \end{array} \right.$$

The following fluxes are used to the resolve the momentum balance equations:

$(G_k)_i^n = (F_k)_i^n \widetilde{(u_k)}_i^n$ where $(F_k)_i^n = \dfrac{1}{2}(F_k)_{i-\frac{1}{2}}^n + \dfrac{1}{2}(F_k)_{i+\frac{1}{2}}^n$ and

$$\widetilde{(u_k)}_i^n = \begin{cases} (u_k)_{i-\frac{1}{2}}^n \ \ if \ \ (F_k)_i^n > 0 \\ (u_k)_{i+\frac{1}{2}}^n \ \ otherwise \end{cases}$$

The momentum balance equations (3.k) are then discretized using the **dual mesh**:

$$h\frac{\Big((\alpha_k\rho_k)_{i+\frac{1}{2}}^{n+1}(u_k)_{i+\frac{1}{2}}^{n+1} - (\alpha_k\rho_k)_{i+\frac{1}{2}}^{n}(u_k)_{i+\frac{1}{2}}^{n}\Big)}{\Delta t} + (G_k)_{i+1}^n - (G_k)_i^n$$

$$+\big[(\alpha_k)_{i+1}^{n+1}(P_k)_{i+1}^{n+1} - (\alpha_k)_i^{n+1}(P_k)_i^{n+1}\big] - (P_I)_{i+\frac{1}{2}}^{n+1}\big[(\alpha_k)_{i+1}^{n+1} - (\alpha_k)_i^{n+1}\big] = 0 \tag{A.5.k}$$

where the approximations of $\alpha_k\rho_k$ and P_I on the dual mesh are defined by $A_{i+\frac{1}{2}}^m := \dfrac{1}{2}A_i^m + \dfrac{1}{2}A_{i+1}^m$ and $(P_k)_i^{n+1} = \mathcal{P}_k((\rho_k)_i^{n+1}, (e_k)_i^{n+1})$

References

[1] R. Abgrall and S. Dallet. An asymptotic preserving scheme for the barotropic Baer-Nunziato model. *Finite Volumes for Complex Applications VII-Elliptic, Parabolic and Hyperbolic Problems*, pages 749–757, 2014.

[2] A. Ambroso, C. Chalons, and P. A. Raviart. A Godunov-type method for the seven-equation model of compressible two-phase flow. *Computers & Fluids*, 54:67–91, 2012.

[3] M. R. Baer and J. W. Nunziato. A two-phase mixture theory for the deflagration-to-detonation transition (DDT) in reactive granular materials. *International journal of multiphase flow*, 12(6):861–889, 1986.

[4] T. Buffard, T. Gallouët, and J. M. Hérard. A sequel to a rough Godunov scheme: application to real gases. *Computers & fluids*, 29(7):813–847, 2000.

[5] F. Coquel, J.M. Hérard, and K. Saleh. A positive and entropy-satisfying finite volume scheme for the baer-nunziato model. *Journal of Computational Physics*, 330, 2017. http://dx.doi.org/10.1016/j.jcp.2016.11.017.

[6] F. Coquel, J.M. Hérard, K. Saleh, and N. Seguin. A robust entropy-satisfying finite volume scheme for the isentropic Baer-Nunziato model. *ESAIM: Math. Model. and Numer. Analysis (M2AN)*, 48:165–206, 2013.

[7] S. Dallet. Phd thesis, to appear (2017).

[8] S. Dallet. Vérification de schémas de convection pour le modèle de Baer-Nunziato. *Internal EDF report*, H-I81-2015-02203-FR, 2015.

[9] E. Franquet and V. Perrier. Runge–Kutta discontinuous Galerkin method for the approximation of Baer and Nunziato type multiphase models. *Journal of Computational Physics*, 231(11):4096–4141, 2012.

[10] T. Gallouët, J.-M. Hérard, and N. Seguin. Numerical modelling of two phase flows using the two fluid two pressure approach. *Mathematical Models and Methods in Applied Sciences*, 14(05):663–700, 2004.

[11] L. Girault and J. M. Hérard. A two-fluid hyperbolic model in a porous medium. *ESAIM: Mathematical Modelling and Numerical Analysis*, 44(06):1319–1348, 2010.

[12] J. Glimm, D. Saltz, and D. Sharp. Renormalization group solution of two-phase flow equations for Rayleigh-Taylor mixing. *Physics Letters A*, 222(3):171–176, 1996.

[13] V. Guillemaud. *Modélisation et simulation numérique des écoulements diphasiques par une approche bifluide à deux pressions*. PhD thesis, Université de Provence-Aix-Marseille I, 2007. https://tel.archives-ouvertes.fr/tel-00169178.

[14] E. Han, M. Hantke, and S. Müller. Modeling of multi-component flows with phase transition and application to collapsing bubbles. *Institut für Geometrie und Praktische Mathematik Preprint*, 409, 2014.

[15] J.-M. Hérard. A three-phase flow model. *Mathematical and computer modelling*, 45(5):732–755, 2007.

[16] R. Herbin, J.-C. Latché, and T.-T. Nguyen. Explicit staggered schemes for the compressible euler equations. *ESAIM: Proceedings*, 40:83–102, 2013.

[17] J. M. Hérard and O. Hurisse. A fractional step method to compute a class of compressible gas–liquid flows. *Computers & Fluids*, 55:57–69, 2012.

[18] P-L. Lions and B. Mercier. Splitting algorithms for the sum of two nonlinear operators. *SIAM Journal on Numerical Analysis*, 16(6):964–979, 1979.

[19] Y. Liu. *Contribution à la vérification et à la validation d'un modèle diphasique bifluide instationnaire*. PhD thesis, Université Aix-Marseille, France, 2013. https://tel.archives-ouvertes.fr/tel-00864567.

[20] S. Müller, M. Hantke, and P. Richter. Closure conditions for non-equilibrium multi-component models. *Continuum Mechanics and Thermodynamics*, pages 1–33, 2015.

[21] V. V. Rusanov. The calculation of the interaction of non-stationary shock waves with barriers. *Zhurnal Vychislitel'noi Matematiki i Matematicheskoi Fiziki*, 1(2):267–279, 1961.

[22] K. Saleh. *Analyse et Simulation Numérique par Relaxation d'Ecoulements Diphasiques Compressibles. Contribution au Traitement des Phases Evanescentes*. PhD thesis, Université Pierre et Marie Curie-Paris VI, France, 2012. https://tel.archives-ouvertes.fr/tel-00761099.

[23] R. Saurel and R. Abgrall. A multiphase Godunov method for compressible multifluid and multiphase flows. *Journal of Computational Physics*, 150(2):425–467, 1999.

[24] D. W. Schwendeman, C. W. Wahle, and A. K. Kapila. The Riemann problem and a high-resolution Godunov method for a model of compressible two-phase flow. *Journal of Computational Physics*, 212(2):490–526, 2006.

[25] S. A. Tokareva and E. F Toro. HLLC-type Riemann solver for the Baer–Nunziato equations of compressible two-phase flow. *Journal of Computational Physics*, 229(10):3573–3604, 2010.